

CLOSED-LOOP NEAR-OPTIMAL SLEW CONTROL USING INTERPOLATION POLYNOMIALS WITHOUT ANGULAR VELOCITY

Sergei Tanygin*

Closed-loop control for a near-optimal slew based on continuously updated 2-point osculating polynomials was recently introduced. This paper employs a similar approach, but modifies it to use only attitude measurements. This eliminates the need to measure or estimate angular velocity making the approach particularly suitable for recently proposed gyro-less spacecraft equipped with high frequency and high accuracy star trackers. Reference slew trajectory is based on Lagrange interpolation polynomials updated periodically with every attitude measurement. Between the updates, the trajectory is guided using angular velocity free control law.

INTRODUCTION

While numerous methods exist for solving the attitude control problem, they generally fall into one of the following categories: some closed-loop controls are developed to ensure asymptotic stability in the presence of initial errors and/or disturbances; others are developed in the framework of the optimal control theory.¹⁻³ Recently proposed closed-loop control based on continuously updated interpolation polynomials provides a simple solution to the attitude control problem, which combines a built-in closed loop with the trajectory that is locally optimal and often globally near-optimal, and that leads to the desired attitude not asymptotically, but in a finite specified time.⁴ 2-point osculating polynomials (Table 1) are of particular interest, because they define least curved trajectories that pass between two points leaving and arriving at specified slopes in specified time (Fig.1).⁴⁻⁷ This property may satisfy the minimum-effort design objective provided that the trajectory curvature can be related to the applied control effort.⁴ For attitude motion, the relationship is complicated due to non-linear kinematics and dynamics involved in mapping of the second derivative of selected attitude parameterization to the applied torque.^{4,8} It was shown that locally optimal closed-loop control law can be developed using 2-point osculating polynomials and rotation vector parameterization:⁴

* Member AAS and AIAA. Lead Engineer, Analytical Graphics, Inc., 40 General Warren Blvd., Malvern, PA 19355, stanygin@stk.com

$$\dot{\bar{\omega}}(t) = \ddot{\bar{\phi}}(t) = 2 \frac{3\phi_T(t) - [2\omega(t) + \dot{\phi}_T(t)](T-t)}{(T-t)^2}, \quad (1)$$

where $\phi_T(t)$ and $\dot{\phi}_T(t)$ are the target rotation vector and its rate relative to the current attitude along the trajectory, $\omega(t)$ is the current angular velocity in the body-fixed frame, $\bar{\omega}(t)$ is the commanded angular acceleration in the body-fixed frame and T is the maneuver duration assuming it started at time 0. When maneuver is relatively short and slow, local optimality translates into approximate global.

Alternatively, this type of optimality can be derived from a different interpolation polynomial, namely a 4-point Lagrange interpolation polynomial (Table 1), which, like its 2-point osculating counterpart, is a cubic. In other words, 4-point Lagrange interpolation polynomials define least curved trajectories that pass through four points at specified times (Fig.1). They are examined closely in this paper as means to eliminate the use of the current angular velocity $\omega(t)$ in the closed loop.

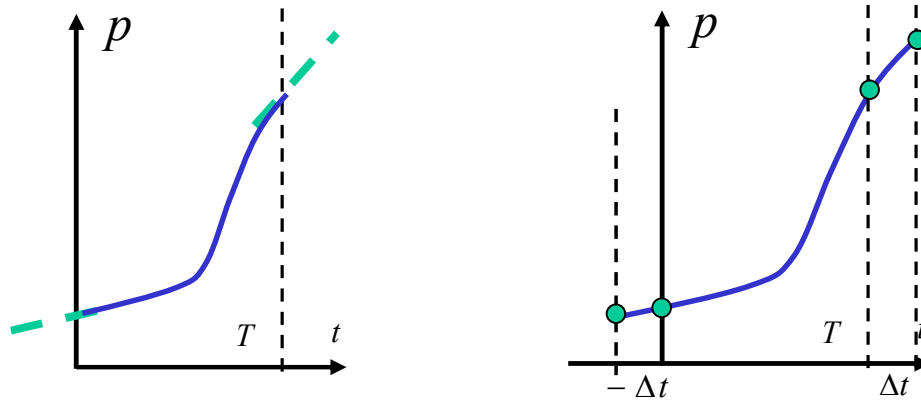


Figure 1 Cubic polynomial $p(t)$ in 2-point osculating and in 4-point Lagrange interpolation

TABLE 1 POLYNOMIAL INTERPOLATION METHODS

	Two points	>Two points
No derivatives	Linear Lagrange	Lagrange
1st derivatives	1st Order Taylor or 2-point Osculating	Osculating
1st and higher derivatives	Taylor	Hermite

Selection of rotation vector for interpolation among various possible attitude parameterizations stems the fact that its Euclidean metric corresponds directly to the eigen-angle between two orientations and that there are no constraints imposed on the elements of this vector. The two properties are important in order to apply and obtain meaningful results from polynomial interpolation of the individual vector elements. Note that the singularities in mapping derivatives of the rotation vector to the body angular velocity and its derivatives that appear when rotation vector is zero are easily resolved:^{4,8}

$$\mathbf{q} = \begin{bmatrix} \hat{\boldsymbol{\phi}} \sin \phi / 2 \\ \cos \phi / 2 \end{bmatrix}, \quad (2)$$

$$\boldsymbol{\omega} = \mathbf{f}(\boldsymbol{\phi}, \dot{\boldsymbol{\phi}}) = [1 - \sin \phi / \phi] (\hat{\boldsymbol{\phi}}^T \dot{\boldsymbol{\phi}}) \hat{\boldsymbol{\phi}} + [\sin \phi / \phi] \dot{\boldsymbol{\phi}} + [(\cos \phi - 1) / \phi] (\hat{\boldsymbol{\phi}} \times \dot{\boldsymbol{\phi}}), \quad (3)$$

$$\begin{aligned} \dot{\boldsymbol{\omega}} = \mathbf{g}(\boldsymbol{\phi}, \dot{\boldsymbol{\phi}}, \ddot{\boldsymbol{\phi}}) = & \ddot{\boldsymbol{\phi}} - (\dot{\phi} / \phi) [\sin \phi / \phi - 2(1 - \cos \phi) / \phi^2] (\hat{\boldsymbol{\phi}} \times \dot{\boldsymbol{\phi}}) \\ & - [(1 - \cos \phi) / \phi] (\hat{\boldsymbol{\phi}} \times \ddot{\boldsymbol{\phi}}) \\ & + (\dot{\phi} / \phi) [(1 - \cos \phi) - 3(1 - \sin \phi / \phi)] \hat{\boldsymbol{\phi}} \times (\hat{\boldsymbol{\phi}} \times \dot{\boldsymbol{\phi}}) \\ & + [(\phi - \sin \phi) / \phi^2] [\phi \hat{\boldsymbol{\phi}} \times (\hat{\boldsymbol{\phi}} \times \ddot{\boldsymbol{\phi}}) + \dot{\boldsymbol{\phi}} \times (\hat{\boldsymbol{\phi}} \times \dot{\boldsymbol{\phi}})] \end{aligned}, \quad (4)$$

where \mathbf{q} is the 4-parameter vector representing the attitude in terms of the unit quaternion, $\boldsymbol{\omega}$ and $\dot{\boldsymbol{\omega}}$ are the body angular velocity and acceleration in the body fixed frame, $\boldsymbol{\phi} = \hat{\boldsymbol{\phi}} \phi$ is the rotation vector with the direction $\hat{\boldsymbol{\phi}}$ along the eigen-axis of rotation relative to the reference frame and with the magnitude ϕ equal to the eigen-angle of rotation. As stated above, these formulas are simplified when rotation vector approaches to or departs from zero, especially if this happens at relatively small rate:

$$\mathbf{q} = \begin{bmatrix} \boldsymbol{\phi} / 2 \\ 0 \end{bmatrix} + o^2(\boldsymbol{\phi}) \quad (5)$$

$$\begin{aligned} \boldsymbol{\omega} = & \dot{\boldsymbol{\phi}} - \frac{\phi}{2} (\hat{\boldsymbol{\phi}} \times \dot{\boldsymbol{\phi}}) + \frac{\phi^2}{6} [(\hat{\boldsymbol{\phi}}^T \dot{\boldsymbol{\phi}}) \hat{\boldsymbol{\phi}} - \dot{\boldsymbol{\phi}}] + o^3(\boldsymbol{\phi}) \\ = & \dot{\boldsymbol{\phi}} - \frac{\phi}{2} (\hat{\boldsymbol{\phi}} \times \dot{\boldsymbol{\phi}}) + o^2(\boldsymbol{\phi}) \end{aligned}, \quad (6)$$

$$\begin{aligned} \dot{\boldsymbol{\omega}} = & \ddot{\boldsymbol{\phi}} - \frac{\phi}{2} (\hat{\boldsymbol{\phi}} \times \ddot{\boldsymbol{\phi}}) + \frac{\phi^2}{6} \hat{\boldsymbol{\phi}} \times (\hat{\boldsymbol{\phi}} \times \ddot{\boldsymbol{\phi}}) \\ & + \frac{\phi \dot{\phi}}{6} (\hat{\boldsymbol{\phi}} \times \dot{\boldsymbol{\phi}}) + \frac{\phi}{6} \dot{\boldsymbol{\phi}} \times (\hat{\boldsymbol{\phi}} \times \dot{\boldsymbol{\phi}}) + o^3(\boldsymbol{\phi}) + o^4(\boldsymbol{\phi}, \dot{\boldsymbol{\phi}}). \\ = & \ddot{\boldsymbol{\phi}} - \frac{\phi}{2} (\hat{\boldsymbol{\phi}} \times \ddot{\boldsymbol{\phi}}) + o^2(\boldsymbol{\phi}) + o^3(\boldsymbol{\phi}, \dot{\boldsymbol{\phi}}) \end{aligned} \quad (7)$$

ROTATION VECTOR INTERPOLATION

It is instructive to review interpolation based control that includes angular velocity before developing one without it. Consider attitude maneuver for which initial and target attitude, initial and target angular velocities, and duration are specified. Minimizing the overall torque spent during the maneuver is certainly one of the most desirable objectives. It was shown that 2-point osculating polynomials produce minimally curved maneuver trajectories in the rotation vector form – the fact that can be approximately related to the overall torque minimization stated above.⁴ However, in the absence of angular velocity measurements, osculating polynomials can not be fully defined. Two alternative approaches to this problem exist: either numerical estimation of angular velocity from attitude measurements or application of Lagrange interpolation, which avoids the use of angular velocity altogether. The former approach effectively leads back to the original problem that includes angular velocity. The latter approach, which is studied in this paper, is different in that it assumes no reliable angular velocity information, either from measurements or from estimates. This also implies that the attitude measurements are available only at discrete times and not continuously, otherwise angular velocity estimates could have been easily extracted from continuous attitude measurements. Points for Lagrange interpolation are selected to satisfy the following criteria: in the limit, formulation for Lagrange interpolation should become equivalent to 2-point osculating interpolation as the sampling period Δt of discrete attitude measurements approaches zero and measurements effectively become continuous; Lagrange interpolation should produce least curved trajectories - the fact that was related to the minimization of the overall torque in the case of 2-point osculating interpolation. Satisfaction of both criteria can be accomplished with 4-point Lagrange interpolation and judicious selection of its control points. Two of the selected points are equivalent to those used in 2-point osculating interpolation – the current attitude measured at time 0 and the target attitude at time T at the end of the maneuver. Two additional points supply information about the shape of the trajectory immediately outside of this time span: at time $-\Delta t$, the latest attitude measurement preceding current measurement; at time $T + \Delta t$, the target attitude at the time of the first measurement after the end of the maneuver (Fig. 1). Similar to a 2-point osculating polynomial, a 4-point Lagrange polynomial is cubic and is constructed as a linear combination of four other cubic polynomials. These polynomials, often referred to as basis, have coefficients that depend only on the time elapsed between the grid points and do not depend on values at the four grid points. Each of the four basis polynomials is then multiplied by corresponding grid point value. These four scaled polynomials added together compose the 4-point Lagrange cubic polynomial. Hence, as in the case of 2-point osculating interpolation, 4-point Lagrange interpolation of the rotation vector $\boldsymbol{\varphi}(t)$ and its derivatives $\dot{\boldsymbol{\varphi}}(t)$, $\ddot{\boldsymbol{\varphi}}(t)$ results in cubic, quadratic and linear polynomials, denoted in this paper $\hat{\boldsymbol{\varphi}}(t)$, $\hat{\dot{\boldsymbol{\varphi}}}(t)$ and $\hat{\ddot{\boldsymbol{\varphi}}}(t)$, respectively. All of them can be formulated as a linear combination of the four other polynomials in the vector form:

$$\widehat{\boldsymbol{\varphi}}(t) = \boldsymbol{\varphi}_- \widehat{p}_-(t) + \boldsymbol{\varphi}_0 \widehat{p}_0(t) + \boldsymbol{\varphi}_T \widehat{p}_T(t) + \boldsymbol{\varphi}_+ \widehat{p}_+(t), \quad (8)$$

$$\dot{\widehat{\boldsymbol{\varphi}}}(t) = \boldsymbol{\varphi}_- \dot{\widehat{p}}_-(t) + \boldsymbol{\varphi}_0 \dot{\widehat{p}}_0(t) + \boldsymbol{\varphi}_T \dot{\widehat{p}}_T(t) + \boldsymbol{\varphi}_+ \dot{\widehat{p}}_+(t), \quad (9)$$

$$\ddot{\widehat{\boldsymbol{\varphi}}}(t) = \boldsymbol{\varphi}_- \ddot{\widehat{p}}_-(t) + \boldsymbol{\varphi}_0 \ddot{\widehat{p}}_0(t) + \boldsymbol{\varphi}_T \ddot{\widehat{p}}_T(t) + \boldsymbol{\varphi}_+ \ddot{\widehat{p}}_+(t), \quad (10)$$

where $\boldsymbol{\varphi}(-\Delta t) = \boldsymbol{\varphi}_-$, $\boldsymbol{\varphi}(0) = \boldsymbol{\varphi}_0$, $\boldsymbol{\varphi}(T) = \boldsymbol{\varphi}_T$, $\boldsymbol{\varphi}(T + \Delta t) = \boldsymbol{\varphi}_+$ and

$$\widehat{p}_-(t) = -\frac{t(t-T)(t-T-\Delta t)}{\Delta t(T+\Delta t)(T+2\Delta t)}, \quad (11)$$

$$\widehat{p}_0(t) = \frac{(t-T)(t-T-\Delta t)(t+\Delta t)}{T\Delta t(T+\Delta t)}, \quad (12)$$

$$\widehat{p}_T(t) = -\frac{t(t+\Delta t)(t-T-\Delta t)}{T\Delta t(T+\Delta t)}, \quad (13)$$

$$\widehat{p}_+(t) = \frac{t(t-T)(t+\Delta t)}{\Delta t(T+\Delta t)(T+2\Delta t)}, \quad (14)$$

$$\dot{\widehat{p}}_-(t) = -\frac{3t^2 - 4Tt + T^2 - \Delta t(2t - T)}{\Delta t(T+\Delta t)(T+2\Delta t)}, \quad (15)$$

$$\dot{\widehat{p}}_0(t) = \frac{3t^2 + T^2 - \Delta t^2 - T(4t + \Delta t)}{T\Delta t(T+\Delta t)}, \quad (16)$$

$$\dot{\widehat{p}}_T(t) = -\frac{3t^2 - T(2t + \Delta t) - \Delta t^2}{T\Delta t(T+\Delta t)}, \quad (17)$$

$$\dot{\widehat{p}}_+(t) = \frac{t(3t + 2\Delta t) - T(2t + \Delta t)}{\Delta t(T+\Delta t)(T+2\Delta t)}, \quad (18)$$

$$\ddot{\widehat{p}}_-(t) = -2\frac{3t - 2T - \Delta t}{\Delta t(T+\Delta t)(T+2\Delta t)}, \quad (19)$$

$$\ddot{\widehat{p}}_0(t) = 2\frac{3t - T}{T\Delta t(T+\Delta t)}, \quad (20)$$

$$\ddot{\widehat{p}}_T(t) = -2\frac{3t - T}{T\Delta t(T+\Delta t)}, \quad (21)$$

$$\ddot{\widehat{p}}_+(t) = 2\frac{3t - T + \Delta t}{\Delta t(T+\Delta t)(T+2\Delta t)}, \quad (22)$$

As stated above, the essential properties of 4-point Lagrange interpolation are $\widehat{\boldsymbol{\varphi}}(-\Delta t) = \boldsymbol{\varphi}(-\Delta t) = \boldsymbol{\varphi}_-$, $\widehat{\boldsymbol{\varphi}}(0) = \boldsymbol{\varphi}(0) = \boldsymbol{\varphi}_0$, $\widehat{\boldsymbol{\varphi}}(T) = \boldsymbol{\varphi}(T) = \boldsymbol{\varphi}_T$, $\widehat{\boldsymbol{\varphi}}(T + \Delta t) = \boldsymbol{\varphi}(T + \Delta t) = \boldsymbol{\varphi}_+$.

In turn, these properties can be deduced from observing the following properties of the basis polynomials:

$$\widehat{p}_0(0) = \widehat{p}_T(T) = \widehat{p}_-(-\Delta t) = \widehat{p}_+(T + \Delta t) = 1, \quad (23)$$

$$\widehat{p}_0(-\Delta t) = \widehat{p}_0(T) = \widehat{p}_0(T + \Delta t) = 0, \quad (24)$$

$$\widehat{p}_T(-\Delta t) = \widehat{p}_T(0) = \widehat{p}_T(T + \Delta t) = 0, \quad (25)$$

$$\widehat{p}_-(0) = \widehat{p}_-(T) = \widehat{p}_-(T + \Delta t) = 0, \quad (26)$$

$$\widehat{p}_+(-\Delta t) = \widehat{p}_+(0) = \widehat{p}_+(T) = 0. \quad (27)$$

In order to illustrate relationship between these polynomials and their 2-point osculating counterparts, it is convenient to introduce pseudo-derivatives based on backward and forward differences at the beginning and at the end of the maneuver, respectively:

$$\delta\boldsymbol{\varphi}_0 = \frac{\boldsymbol{\varphi}_0 - \boldsymbol{\varphi}_-}{\Delta t}, \quad (28)$$

$$\delta\boldsymbol{\varphi}_T = \frac{\boldsymbol{\varphi}_+ - \boldsymbol{\varphi}_T}{\Delta t}. \quad (29)$$

Then, using

$$\widetilde{p}_0(t) = \widehat{p}_0(t) + \widehat{p}_-(t), \quad (30)$$

$$\widetilde{r}_0(t) = -\widehat{p}_-(t)\Delta t, \quad (31)$$

$$\widetilde{p}_T(t) = \widehat{p}_T(t) + \widehat{p}_+(t), \quad (32)$$

$$\widetilde{r}_T(t) = \widehat{p}_+(t)\Delta t, \quad (33)$$

interpolated trajectory and its derivatives (Eqs.(8-10)) become

$$\widehat{\boldsymbol{\varphi}}(t) = \boldsymbol{\varphi}_0\widetilde{p}_0(t) + \delta\boldsymbol{\varphi}_0\widetilde{r}_0(t) + \boldsymbol{\varphi}_T\widetilde{p}_T(t) + \delta\boldsymbol{\varphi}_T\widetilde{r}_T(t), \quad (34)$$

$$\dot{\widehat{\boldsymbol{\varphi}}}(t) = \boldsymbol{\varphi}_0\dot{\widetilde{p}}_0(t) + \delta\boldsymbol{\varphi}_0\dot{\widetilde{r}}_0(t) + \boldsymbol{\varphi}_T\dot{\widetilde{p}}_T(t) + \delta\boldsymbol{\varphi}_T\dot{\widetilde{r}}_T(t), \quad (35)$$

$$\ddot{\widehat{\boldsymbol{\varphi}}}(t) = \boldsymbol{\varphi}_0\ddot{\widetilde{p}}_0(t) + \delta\boldsymbol{\varphi}_0\ddot{\widetilde{r}}_0(t) + \boldsymbol{\varphi}_T\ddot{\widetilde{p}}_T(t) + \delta\boldsymbol{\varphi}_T\ddot{\widetilde{r}}_T(t), \quad (36)$$

where, using $t = \tau\Delta t$ and $\Delta t = \lambda T$,

$$\widetilde{p}_0(t) = \frac{(1 - \tau\lambda)(1 + \lambda - \tau\lambda)(1 + 2\lambda + 2\tau\lambda)}{(1 + \lambda)(1 + 2\lambda)}, \quad (37)$$

$$\widetilde{r}_0(t) = \frac{\tau\lambda(1 - \tau\lambda)(1 + \lambda - \tau\lambda)}{(1 + \lambda)(1 + 2\lambda)}T, \quad (38)$$

$$\tilde{p}_T(t) = \frac{\tau(1+\tau)\lambda^2(3+2\lambda-2\tau\lambda)}{(1+\lambda)(1+2\lambda)}, \quad (39)$$

$$\tilde{r}_T(t) = -\frac{\tau(1+\tau)\lambda^2(1-\tau\lambda)}{(1+\lambda)(1+2\lambda)}T, \quad (40)$$

$$\dot{\tilde{p}}_0(t) = -\frac{\lambda(3+6\tau+2\lambda-6\tau^2\lambda)}{(1+\lambda)(1+2\lambda)}\frac{1}{T}, \quad (41)$$

$$\dot{\tilde{r}}_0(t) = \frac{1+\lambda-4\tau\lambda-2\tau\lambda^2+3\tau^2\lambda^2}{(1+\lambda)(1+2\lambda)}, \quad (42)$$

$$\dot{\tilde{p}}_T(t) = \frac{\lambda(3+6\tau+2\lambda-6\tau^2\lambda)}{(1+\lambda)(1+2\lambda)}\frac{1}{T}, \quad (43)$$

$$\dot{\tilde{r}}_T(t) = -\frac{\lambda(1+2\lambda-2\tau\lambda-3\tau^2\lambda)}{(1+\lambda)(1+2\lambda)}, \quad (44)$$

$$\ddot{\tilde{p}}_0(t) = -\frac{3(1-2\tau\lambda)}{(1+\lambda)(1+2\lambda)}\frac{2}{T^2}, \quad (45)$$

$$\ddot{\tilde{r}}_0(t) = -\frac{2(2+\lambda-3\tau\lambda)}{(1+\lambda)(1+2\lambda)}\frac{1}{T}, \quad (46)$$

$$\ddot{\tilde{p}}_T(t) = \frac{3(1-2\tau\lambda)}{(1+\lambda)(1+2\lambda)}\frac{2}{T^2}, \quad (47)$$

$$\ddot{\tilde{r}}_T(t) = -\frac{2(1-\lambda-3\tau\lambda)}{(1+\lambda)(1+2\lambda)}\frac{1}{T}. \quad (48)$$

The basis polynomials restated in this form do not exhibit singularities as the sampling period Δt approaches zero. In fact, these polynomials approach their 2-point osculating counterparts,⁴ thus, satisfying the criterion of their equivalence as $\Delta t \rightarrow 0$.

NEAR OPTIMAL FIXED DURATION MANEUVER

The design of interpolation based closed-loop control using only discrete attitude measurements follows closely a similar design for continuous control. Recall that the attitude maneuver with discrete measurements is defined by four points and that the objective is to minimize the overall torque spent during the maneuver. The design is based on a mapping of the rotation vector and its derivatives evaluated along the interpolated trajectory to the body angular velocity and acceleration, and ultimately, to the applied torque.

Note that:

1. At specified times, trajectory passes through four points, the beginning and the end of the maneuver as well as the points immediately outside of the maneuver time span
2. Trajectory is least curved in rotation vector parameterization

The first property comes directly from Lagrange interpolation itself as developed in the previous section. The second property comes from using calculus of variations to minimize the following objective functions:

$$J(\phi_i) = \int_0^T \ddot{\phi}_i^2 dt, i = 1, 2, 3, \quad (49)$$

where $\phi_i \in \mathfrak{R}^1$ is the i th element of the rotation vector $\boldsymbol{\phi}$. The Euler-Lagrange equation^{9,10} yields the following condition for ϕ_i :^{4,7}

$$\overset{\dots}{\phi}_i \equiv 0, i = 1, 2, 3, \quad (50)$$

which is clearly satisfied whenever ϕ_i is a cubic polynomial.⁴ Hence, similar to 2-point osculating polynomials, the 4-point Lagrange polynomials $\widehat{\phi}_i$ defined in the previous section as elements of $\widehat{\boldsymbol{\phi}} = [\widehat{\phi}_1 \quad \widehat{\phi}_2 \quad \widehat{\phi}_3]^T$, minimize the objective functions

$$\min_{\phi_i} J(\phi_i) = J(\widehat{\phi}_i), i = 1, 2, 3. \quad (51)$$

A closer examination of rotational kinematics and dynamics is needed in order to relate this result to the ultimate objective function:

$$J_M(\boldsymbol{\phi}) = \int_0^T \mathbf{M}^T \mathbf{M} dt, \quad (52)$$

where $\mathbf{M} \in \mathfrak{R}^3$ is the applied torque. The rotational dynamics written in the body fixed frame with respect to some inertial frame define nonlinear relationship between the angular velocity and the applied torque:^{3,8}

$$\mathbf{M}(t) = \mathbf{I}\dot{\boldsymbol{\omega}}(t) + \boldsymbol{\omega}(t) \times \mathbf{I}\boldsymbol{\omega}(t) + \boldsymbol{\omega}(t) \times \mathbf{h}(t), \quad (53)$$

where $0 < \mathbf{I} = \mathbf{I}^T \in \mathfrak{R}^{3 \times 3}$ is the body inertia matrix and $\mathbf{h} \in \mathfrak{R}^3$ is the momentum bias. The fact that any inertial frame is valid as a reference for the rotational dynamics can be exploited to simplify the rotational kinematics. Aligning the reference inertial frame with

the current attitude measurement results in a small eigen-angle ϕ in the vicinity of the measurement in which case the dynamics can be restated as

$$\mathbf{M}(t) = \mathbf{I}\ddot{\boldsymbol{\varphi}}(t) + \boldsymbol{\omega}(t) \times \mathbf{I}\boldsymbol{\omega}(t) + \boldsymbol{\omega}(t) \times \mathbf{h}(t) + o(\boldsymbol{\varphi}). \quad (54)$$

There are several well known conditions under which the gyroscopic coupling term $\boldsymbol{\omega}(t) \times \mathbf{I}\boldsymbol{\omega}(t) + \boldsymbol{\omega}(t) \times \mathbf{h}(t)$ can be neglected, e.g. a slow rotation or a rotation near one of the principal axes in the absence of momentum bias. It is under these conditions that the rotation vector trajectory $\widehat{\boldsymbol{\varphi}}$ in the form of 4-point Lagrange polynomials approximately minimizes the desired objective function

$$\min_{\boldsymbol{\varphi}} J_M(\boldsymbol{\varphi}) \approx J_M(\widehat{\boldsymbol{\varphi}}) \quad (55)$$

and it does so locally in the vicinity of the current attitude measurement, i.e. when $\phi \ll 1$. This localization can be maintained by re-stating the problem relative to each new attitude measurement provided that the measurements become available within a sufficiently small period (Fig.2).

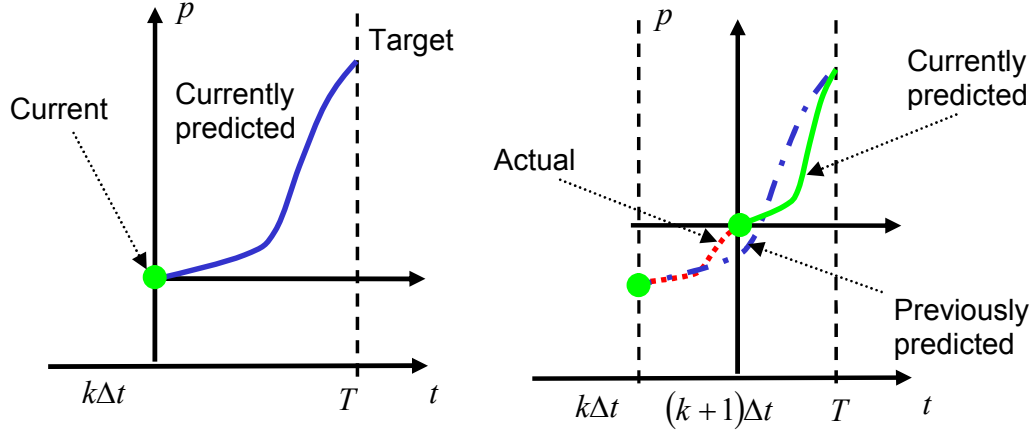


Figure 2 Targeting using periodically updated interpolation polynomials $p(t)$

This iterative method can be described using index notation with the total number of measurements during the maneuver, N , such that $T = N\Delta t$, and with the current measurement index, k , such that $k = 0, 1, 2, \dots, N-1$:

$$\widehat{\boldsymbol{\varphi}}_{k|k+1}(t) = \delta\boldsymbol{\varphi}_{k|k}\tilde{r}_{k|k}(t) + \boldsymbol{\varphi}_{k|N}\tilde{p}_{k|N}(t) + \delta\boldsymbol{\varphi}_{k|N}\tilde{r}_{k|N}(t), \quad (56)$$

$$\dot{\widehat{\boldsymbol{\varphi}}}_{k|k+1}(t) = \delta\dot{\boldsymbol{\varphi}}_{k|k}\tilde{r}_{k|k}(t) + \boldsymbol{\varphi}_{k|N}\dot{\tilde{p}}_{k|N}(t) + \delta\dot{\boldsymbol{\varphi}}_{k|N}\tilde{r}_{k|N}(t), \quad (57)$$

$$\ddot{\widehat{\boldsymbol{\varphi}}}_{k|k+1}(t) = \delta\ddot{\boldsymbol{\varphi}}_{k|k}\tilde{r}_{k|k}(t) + \boldsymbol{\varphi}_{k|N}\ddot{\tilde{p}}_{k|N}(t) + \delta\ddot{\boldsymbol{\varphi}}_{k|N}\tilde{r}_{k|N}(t). \quad (58)$$

These formulas define the desired rotation vector $\hat{\boldsymbol{\varphi}}$, its velocity $\dot{\hat{\boldsymbol{\varphi}}}$ and acceleration $\ddot{\hat{\boldsymbol{\varphi}}}$ for the period between measurements k and $k+1$. The trajectory is defined relative to measurement k , which is why $\boldsymbol{\varphi}_{k|k} \equiv 0$. Note that $\boldsymbol{\varphi}_{k|N}$ and $\delta\boldsymbol{\varphi}_{k|N}$ represent the end-of-maneuver target rotation vector and its forward difference pseudo-derivative defined relative to the inertial frame aligned with measurement k , whereas $\delta\boldsymbol{\varphi}_{k|k}$ represents current backward difference pseudo-derivative based on measurements $k-1$ and k also defined relative to the same inertial frame. Similarly, the basis polynomials and their derivatives are constructed for the time span between measurements k and N . The commanded torque for the period between measurements k and $k+1$ becomes

$$\hat{\mathbf{M}}(t) = \mathbf{I}\hat{\boldsymbol{\omega}}(t) + \hat{\boldsymbol{\omega}}(t) \times \mathbf{I}\hat{\boldsymbol{\omega}}(t) + \hat{\boldsymbol{\omega}}(t) \times \mathbf{h}(t), \quad (59)$$

where desired angular velocity and acceleration are computed based on their kinematical relationships to rotation vector and its derivatives (Eqs.(3,4)), i.e. $\hat{\boldsymbol{\omega}}(t) = \mathbf{f}(\hat{\boldsymbol{\varphi}}(t), \dot{\hat{\boldsymbol{\varphi}}}(t))$ and $\ddot{\hat{\boldsymbol{\omega}}}(t) = \mathbf{g}(\hat{\boldsymbol{\varphi}}(t), \dot{\hat{\boldsymbol{\varphi}}}(t), \ddot{\hat{\boldsymbol{\varphi}}}(t))$. In summary, the periodically updated interpolation polynomials (Eqs.(56-58)), the rotation vector kinematics (Eqs.(3,4)) and the commanded torque formulation (Eq.(59)) presented in this section constitute a hybrid closed-loop guidance law that uses periodic attitude only measurements along with continuous commanded torque in order to pass through two desired attitudes: one at the specified end of the maneuver and the other at the time of the next measurement after the maneuver. Also, the closed-loop trajectory is locally optimal and is overall near optimal for relatively small and slow maneuvers.

PARAMETER SENSITIVITY AND STABILITY ANALYSIS

Any practical use of the hybrid closed-loop approach for performing attitude maneuvers proposed in the previous section depends on how sensitive it is to variations in the initial and target conditions, in the sampling period and in other parameters. The analysis can be separated in two parts: sensitivity of the interpolated trajectory itself and stability of the actual closed-loop trajectory designed to follow it.

Recall that, at any time, the interpolated trajectory is fully defined by its four control points: the two latest attitude measurements, the target attitude at the end of the maneuver and the target attitude at the time of the measurement immediately after the maneuver. Since interpolated rotation vector trajectory and its derivatives are known in closed form (Eqs.(56-58)), sensitivities can be easily derived using analytic partial derivatives with respect to the control points. Note that the interpolated trajectory is updated after every measurement so that only the initial part of the trajectory is used limited in duration to the sampling period. Of course, as the end of the maneuver nears, the ratio λ of the sampling period with the remaining maneuver time span grows, eventually reaching 100% at the last measurement before the maneuver end. Also, note that the influence of the rotation vector acceleration on the commanded torque is

dominant for relatively slow and well sampled maneuvers. This is why, in the interest of brevity, this paper only describes sensitivity to interpolation control points for the rotation vector acceleration. The scaled sensitivities to the initial rotation vector difference (slope), the overall rotation vector displacement and the final slope are characterized as follows:

$$\mathbf{S}_{\mathbf{r}_{k|k}} = \max_{\tau \in [0,1]} \left| \frac{\partial \ddot{\Phi}_{k|k+1}}{\partial \delta \Phi_{k|k}} \right| T = \text{diag} \left[\max_{\tau \in [0,1]} \left| \ddot{r}_{k|k} \right| \right] T, \quad (60)$$

$$\mathbf{S}_{\mathbf{p}_{k|N}} = \max_{\tau \in [0,1]} \left| \frac{\partial \ddot{\Phi}_{k|k+1}}{\partial \Phi_{k|N}} \right| \frac{T^2}{2} = \text{diag} \left[\max_{\tau \in [0,1]} \left| \ddot{p}_{k|N} \right| \right] \frac{T^2}{2}, \quad (61)$$

$$\mathbf{S}_{\mathbf{r}_{k|N}} = \max_{\tau \in [0,1]} \left| \frac{\partial \ddot{\Phi}_{k|k+1}}{\partial \delta \Phi_{k|N}} \right| T = \text{diag} \left[\max_{\tau \in [0,1]} \left| \ddot{r}_{k|N} \right| T \right]. \quad (62)$$

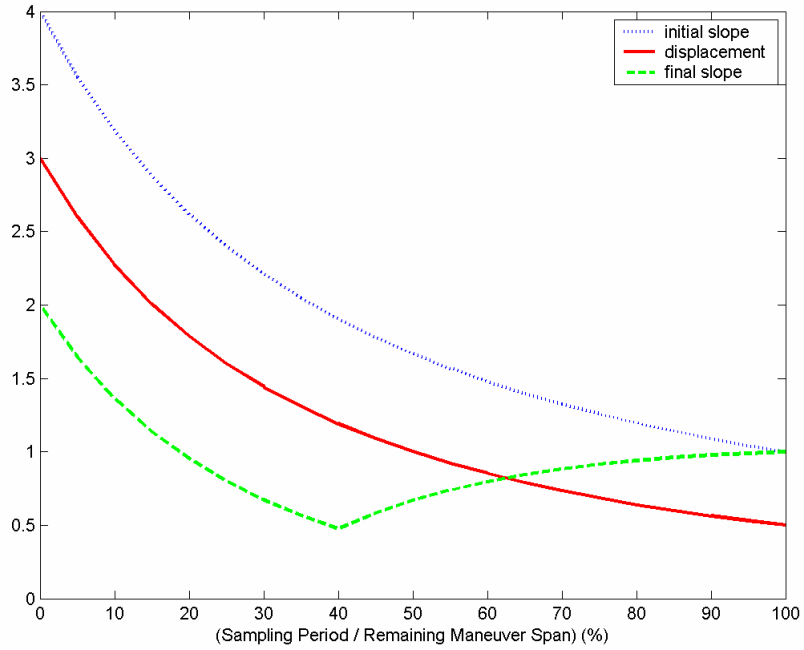


Figure 3 Scaled sensitivity of rotation vector acceleration

The results (Fig.3) indicate that the rotation vector acceleration along the interpolated trajectory becomes less sensitive to the interpolation control points as the maneuver progresses. This effect improves robustness of the trajectory, because it counteracts the fact that a smaller remaining maneuver span leaves a shorter time to correct any trajectory errors. However, even at the beginning of the maneuver, when the sampling period may represent only a small portion of the overall time span, the sensitivities are no

more than four times larger than those that would have been observed if a constant acceleration trajectory were required to pass through any one of the control points.

The second part of the analysis deals with the fact that, even if the interpolated trajectory is well behaved, the actual closed-loop trajectory may not be. The primary source of errors between the interpolated and actual trajectories lies in the difference between the angular velocities along the two trajectories. Note that the angular velocity difference is not measured and, thus, is not explicitly controlled. Instead, it is detected indirectly via the difference between predicted and actual attitude measurements at sampling times. In the limit, when sampling period approaches zero, sampling becomes effectively continuous and angular velocity difference vanishes. Otherwise, the predicted angular velocity is used to construct the commanded torque (Eq.(59)) and angular velocity error dynamics takes on the following form:

$$\mathbf{I}\dot{\boldsymbol{\varepsilon}}(t) + \boldsymbol{\varepsilon}(t) \times \mathbf{I}\boldsymbol{\omega}(t) + \boldsymbol{\omega}(t) \times \mathbf{I}\boldsymbol{\varepsilon}(t) + \boldsymbol{\varepsilon}(t) \times \mathbf{h}(t) = 0, \quad (63)$$

where $\boldsymbol{\varepsilon}(t) = \widehat{\boldsymbol{\omega}}(t) - \boldsymbol{\omega}(t)$. The analysis of the region of stability in this case is the subject of future research. This paper provides several numerical examples that illustrate behavior of the angular velocity error.

EXAMPLES

This section illustrates a performance of the closed-loop guidance law using only periodic attitude measurements. The following characteristics are common for all cases considered:

- Maneuver start time: 10s
- Attitude measurements sampling period: $\Delta t = 1s$
- Body is rigid and is without momentum bias
- Initial quaternion and target quaternion:

$$\mathbf{q}(0s) = [0 \quad 0 \quad 1 \quad 0]^T$$

$$\mathbf{q}(180s) = [-0.3829 \quad -0.6621 \quad 0.4139 \quad 0.4936]^T$$

The first case deals with a fully symmetric body thus avoiding gyroscopic coupling. The motion starts with the angular velocity

$$\boldsymbol{\omega}(0s) = [0 \quad 0 \quad 0.055]^T \text{ deg/s}$$

and targets attitude one second after the maneuver to be

$$\mathbf{q}(181s) = [-0.3840 \quad -0.6675 \quad 0.4101 \quad 0.4886]^T.$$

The second and third cases deal with a more agile maneuver that starts with a larger angular velocity

$$\boldsymbol{\omega}(0s) = [5.550 \quad 0 \quad 0.055]^T \text{ deg/s}$$

and targets attitude one second after the maneuver to be

$$\mathbf{q}(181s) = [-0.3923 \quad -0.7095 \quad 0.3784 \quad 0.4468]^T,$$

which, compared with the first case, is also further away from the end-of-maneuver attitude. In addition, the third case no longer uses a symmetric body: it uses the body with the following inertia matrix:

$$\mathbf{I} = \begin{bmatrix} 4500 & 0 & 0 \\ 0 & 2500 & 0 \\ 0 & 0 & 1500 \end{bmatrix} \text{ kgm}^2,$$

thus, introducing gyroscopic coupling.

The kinematical performance measure related to the minimization of the applied torque is defined as follows:

$$Jr(t) = \int_0^t \sqrt{\dot{\boldsymbol{\omega}}^T \dot{\boldsymbol{\omega}}} d\tau. \quad (64)$$

Performance of the first maneuver is illustrated by time history of the error eigen-angle relative to the target attitude (Figs. 4, 5). The angle decreases steadily and almost linearly, because both the initial and final angular velocities are relatively small. The target attitude at the end of the maneuver is reached with very good accuracy and, while the error angle grows after that, it is still less than 0.01% of the total maneuver angle at the next measurement time (Fig. 5). Similarly, the performance measure $Jr(t)$ exhibits slightly curved but close to linear behavior during the maneuver (Fig. 6).

For the second and third maneuvers, the error angle relative to the target attitude exhibits a much more pronounced non-linear behavior due to the higher initial and final angular velocities (Figs. 7, 8). The effect of gyroscopic coupling introduced in the third maneuver appears to be limited. However, it is clear that, at the first measurement time after the end of the maneuver, the error is larger during the maneuver with the asymmetric body (Fig. 8). In order to support parameter sensitivity and stability analysis, the errors between the interpolated and actual angular velocities are recorded (Figs. 9, 10). The errors are generally quite small with two spikes corresponding to the maneuver initial phase and to the phase during at which the angular velocity direction undergoes fast transitions in the body frame (at about 120s) (Fig. 10). The errors between the interpolated and actual angular accelerations exhibit entirely similar behavior, but on a

smaller scale (Figs. 11, 12). Note that additional insight into attitude trajectory evolution can be gained from using 3-dimensional visualization of body frame axes (Fig. 13) as well as of other vectors.

CONCLUSIONS

The paper formulates the 4-point Lagrange interpolation problem for attitude using rotation vector parameterization. The paper demonstrates that the resulting interpolated trajectory can serve as the fixed time attitude maneuver trajectory, for which minimization of the overall applied torque is investigated as the optimality criterion. The paper establishes that the trajectory is locally optimal and can be near-optimal overall for relatively small and slow maneuvers. The paper extends recently proposed closed-loop guidance approach based on continuously updated interpolated trajectories. The extension seeks to enable interpolation based maneuvers for gyro-less spacecraft, which produce high frequency and high accuracy attitude measurements, but no angular velocity measurements for closed-loop control¹¹⁻¹³. The paper demonstrates that interpolated maneuver trajectories can be both defined and updated periodically without angular velocity measurements. This serves as a foundation for the development of hybrid guidance approach using periodic attitude measurements and continuous control. Numerical simulations illustrate viability of the proposed maneuver design.

REFERENCES

1. J.L. Junkins and J.D. Turner, "Optimal Continuous Torque Attitude Maneuvers," *Journal of Guidance, Control and Dynamics*, Vol.3, No. 3, 1980, pp.210-217.
2. J.L. Junkins, *Optimal Spacecraft Rotational Maneuvers*, Studies in Astronautics, Vol.3, 1986.
3. B. Wie, *Space Vehicle Dynamics and Control*, AIAA Education Series, 1998.
4. S. Tanygin, "Attitude Interpolation," Paper AAS 03-197, AAS/AIAA Space Flight Mechanics Meeting, Ponce, Puerto-Rico, Feb. 2003.
5. P.J. Davis, *Interpolation and Approximation*, Dover Publications Inc., New York, 1975, pp.24-55.
6. K. Shoemake, "Animation Rotation with Quaternion Curves," *Computer Graphics*, Vol.19(3), 1985, pp. 245-254.
7. A.H. Barr, B. Currin, S. Gabriel, and J.F. Hughes, "Smooth Interpolation of Orientations with Angular Velocity Constraints using Quaternions," *SIGGRAPH' 92 Proceedings*, 1992, pp. 313-320.

8. M.D. Shuster, "A Survey of Attitude Representations," *Journal of the Astronautical Sciences*, Vol.41, No.4, 1993, pp.439-517.
9. D. Zwillinger, *Handbook of Differential Equations*, 2nd Ed., Academic Press Inc., New York, 1992, pp. 5, 7, 88-93.
10. D. A. Pierre, *Optimization Theory with Applications*, Dover Publications Inc., New York, 1986, pp. 45-46, 62-75.
11. P.Singla, J.L. Crassidis and J.L. Junkins, "Spacecraft Angular Rate Estimation Algorithms for A Star Tracker Mission," Paper AAS 03-191, AAS/AIAA Space Flight Mechanics Meeting, Ponce, Puerto-Rico, Feb. 2003.
12. M.R. Akella, "Rigid Body Attitude Tracking without Angular Velocity Feedback," *Systems and Control Letters*, Vol.42, 2001, pp.321-326.
13. S. Tanygin, "Generalization of Adaptive Attitude Tracking," AIAA/AAS Astrodynamics Specialist Conference, 2002.

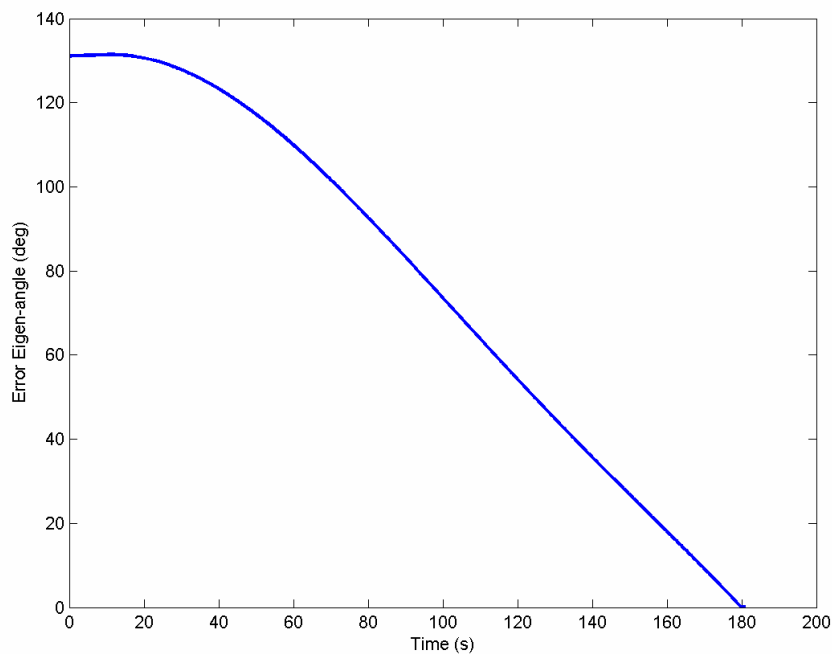


Figure 4 Error eigen-angle relative to target attitude

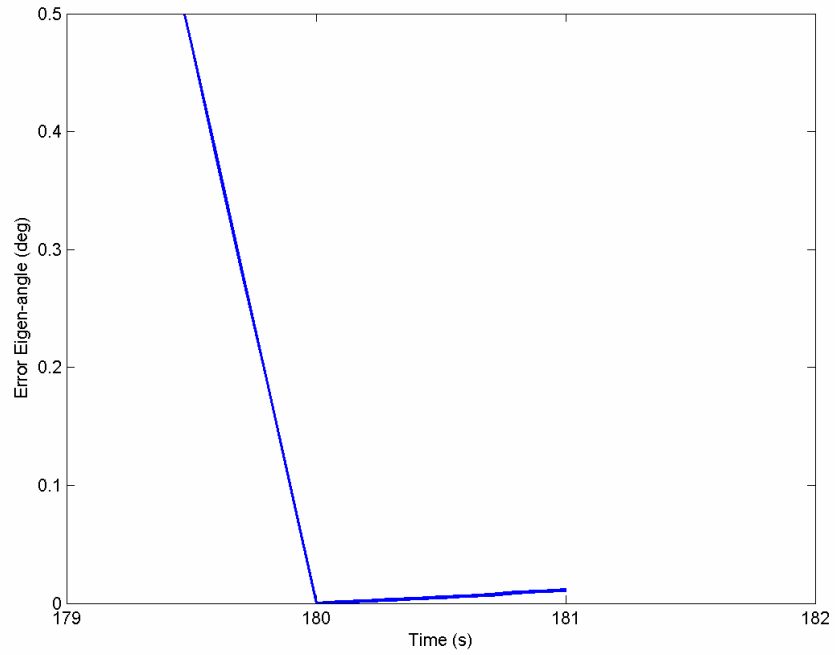


Figure 5 Error eigen-angle relative to target attitude at maneuver end

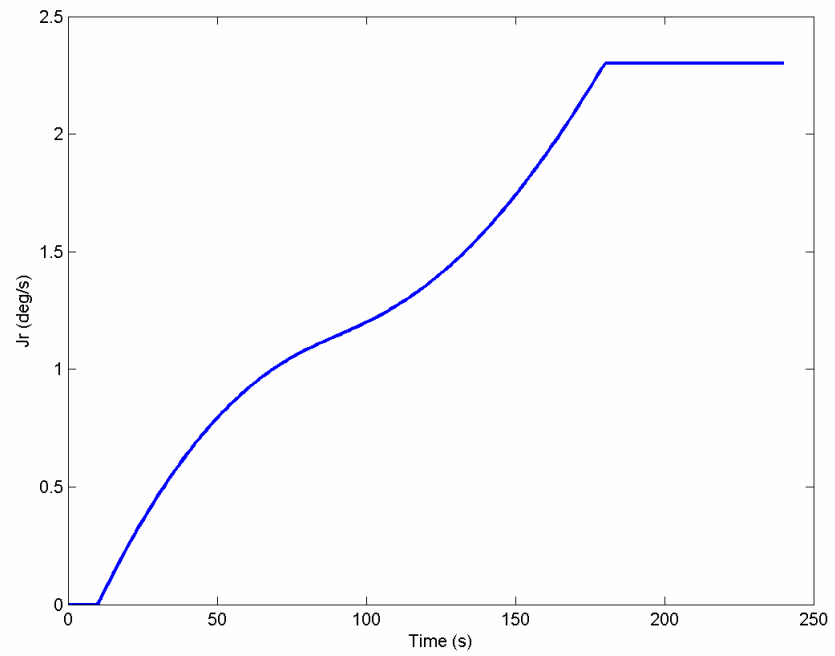


Figure 6 Performance measure

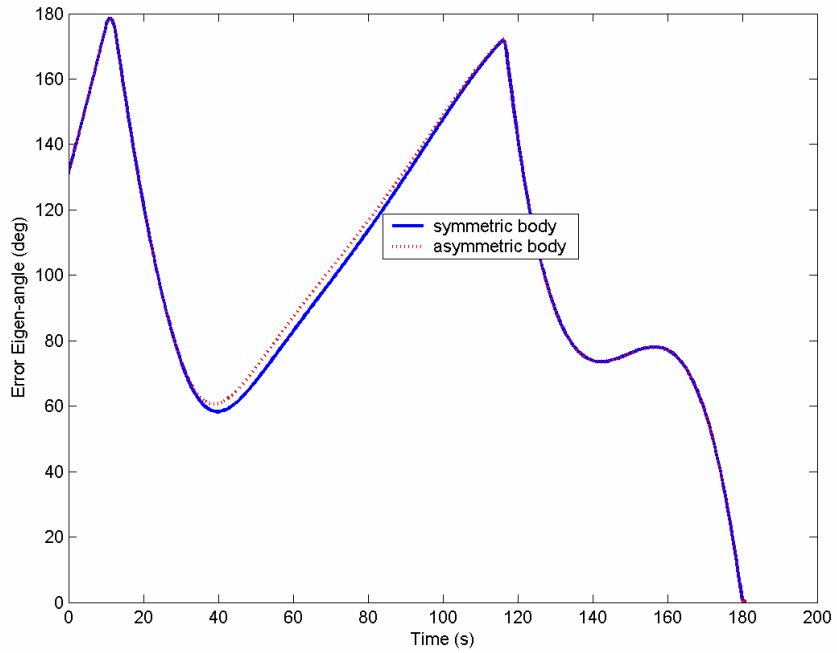


Figure 7 Error eigen-angle relative to target attitude

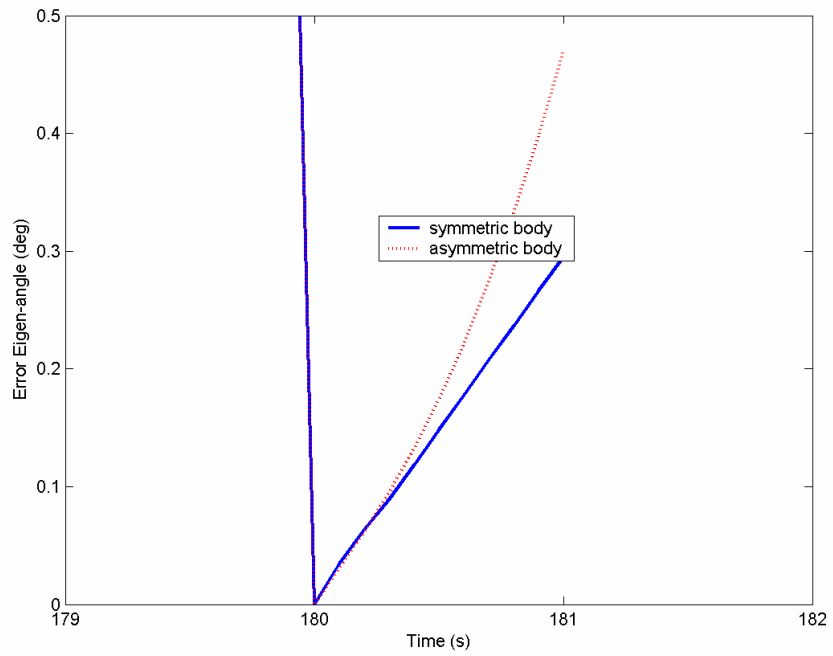


Figure 8 Error eigen-angle relative to target attitude at maneuver end

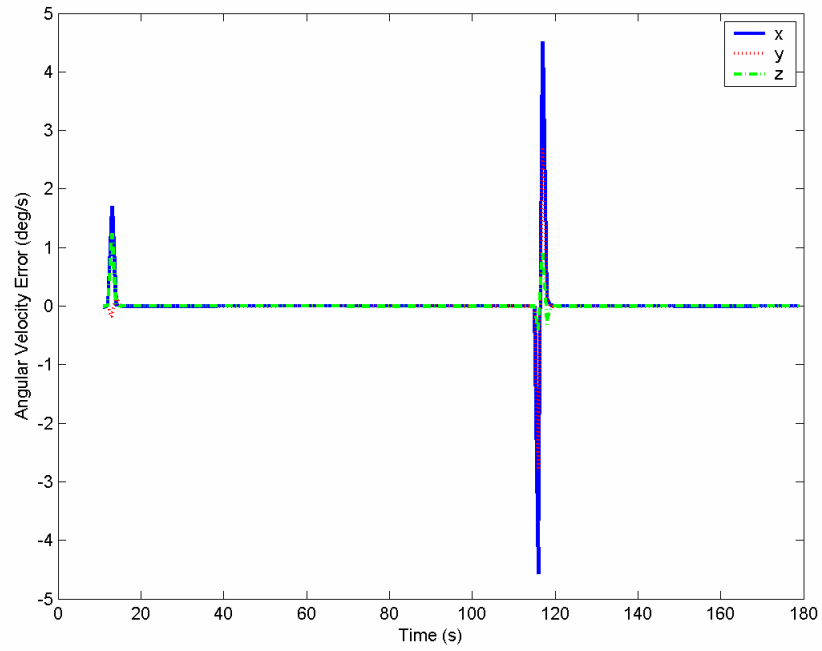


Figure 9 Error between desired and actual angular velocities

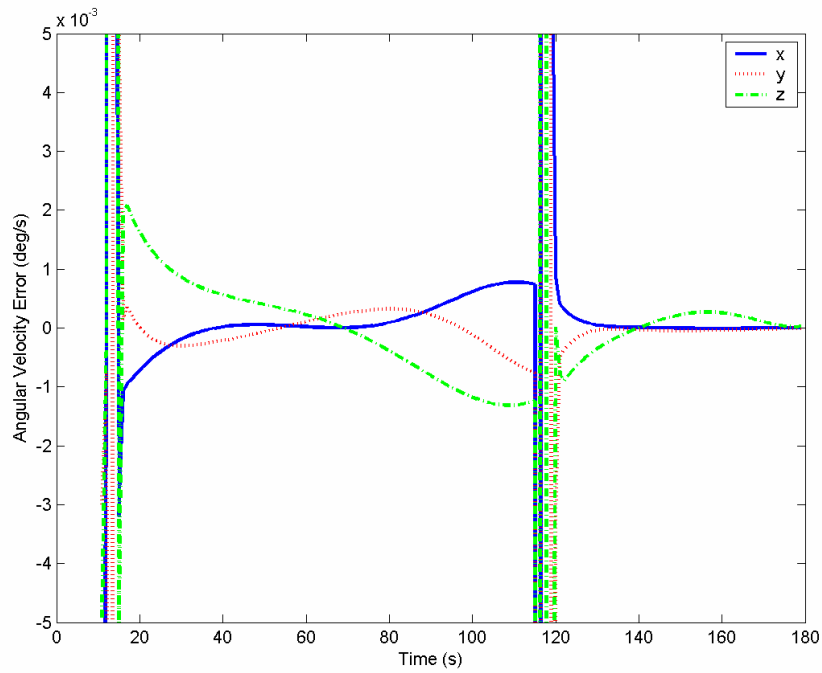


Figure 10 Small scale error between desired and actual angular velocities

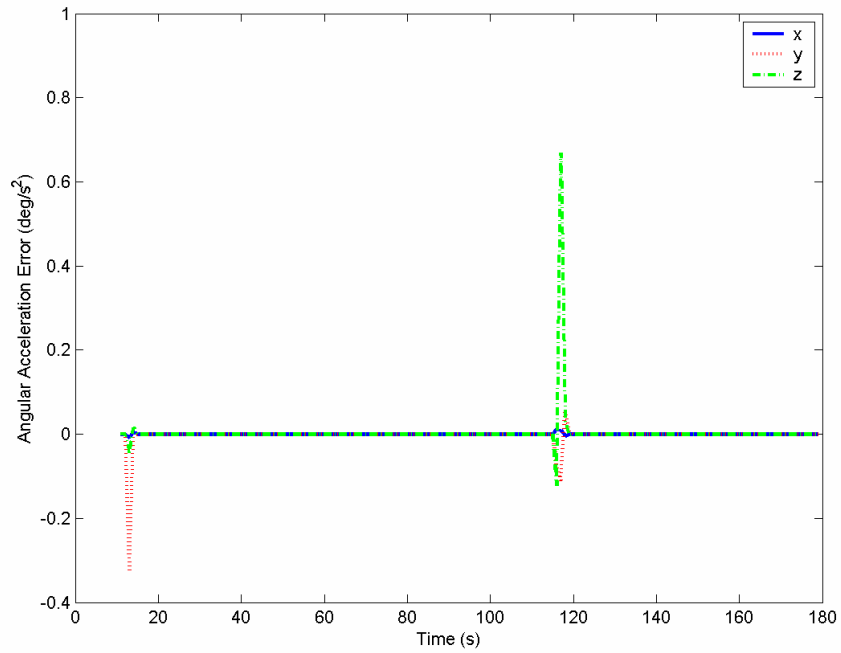


Figure 11 Error between desired and actual angular accelerations

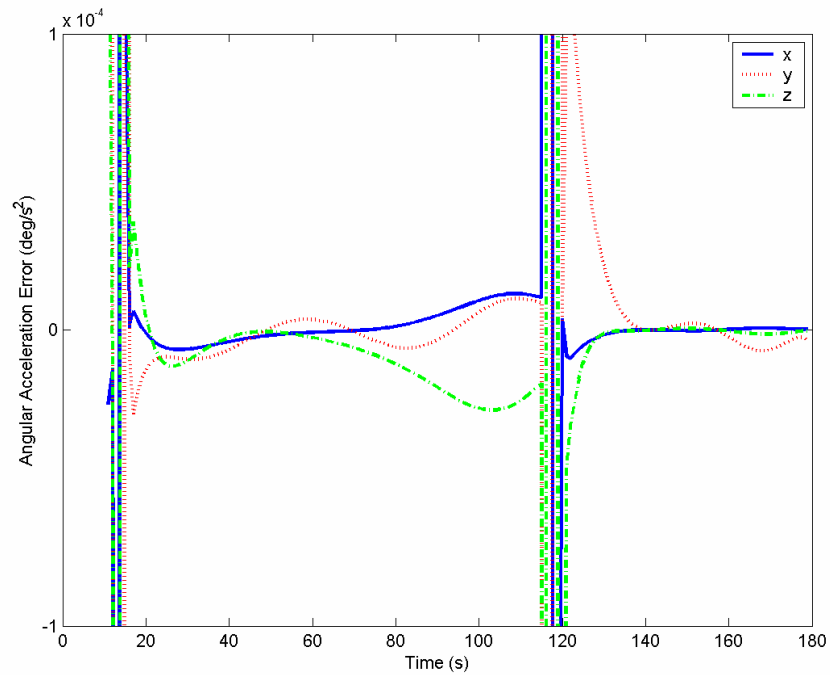


Figure 12 Small scale error between desired and actual angular accelerations

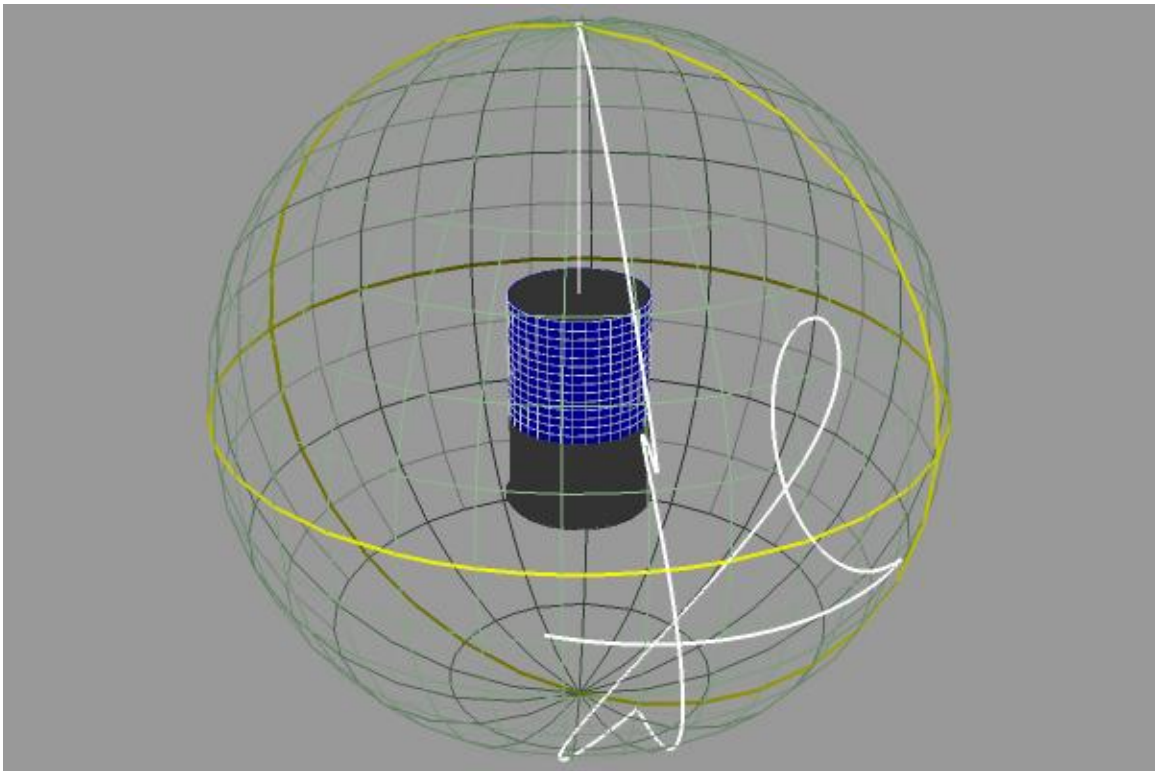


Figure 13 Motion of body frame Z-axis during agile maneuver